Lipid−Protein Interactions Studied by Introduction of a Tryptophan Residue: The Mechanosensitive Channel MscL[†]

Andrew M. Powl, J. Malcolm East, and Anthony G. Lee*

Division of Biochemistry and Molecular Biology, School of Biological Sciences, University of Southampton, Southampton SO16 7PX, U.K.

Received June 11, 2003; Revised Manuscript Received September 30, 2003

ABSTRACT: Trp fluorescence spectroscopy is a powerful tool to study the structures of membrane proteins and their interactions with the surrounding lipid bilayer. Many membrane proteins contain more than one Trp residue, making analysis of the fluorescence data more complex. The mechanosensitive channels MscL's of *Mycobacterium tuberculosis* (TbMscL) and *Escherichia coli* (EcMscL) contain no Trp residues. We have therefore introduced single Trp residues into the transmembrane regions of TbMscL and EcMscL to give the Trp-containing mutants F80W-TbMscL and F93W-EcMscL, respectively, which we show are highly suitable for measurements of lipid binding constants. In vivo cell viability assays in *E. coli* show that introduction of the Trp residues does not block function of the channels. The Trp-containing mutants have been reconstituted into lipid bilayers by mixing in cholate followed by dilution to re-form membranes. Cross-linking experiments suggest that the proteins retain their pentameric structures in phosphatidylcholines with chain lengths between C14 and C24, phosphatidylserines, and phosphatidic acid. Quenching of Trp fluorescence by brominated phospholipids suggests that the Trp residue in F80W-TbMscL is more exposed to the lipid bilayer than the Trp residue in F93W-EcMscL. Binding constants for phosphatidylcholines change with changing fatty acyl chain length, the strongest interaction for both TbMscL and EcMscL being observed with a chain of length C16, corresponding to a bilayer of hydrophobic thickness ca. 24 Å, compared to a hydrophobic thickness for TbMscL of about 26 Å estimated from the crystal structure. Lipid binding constants change by only a factor of 1.5 in the chain length range from C12 to C24, much less than expected from theories of hydrophobic mismatch in which the protein is treated as a rigid body. It is concluded that MscL distorts to match changes in bilayer thickness. The binding constants for dioleoylphosphatidylethanolamine for both TbMscL and EcMscL relative to those for dioleoylphosphatidylcholine are close to 1. Quenching experiments suggest a single class of binding sites for phosphatidylserine, phosphatidylglycerol, and cardiolipin on TbMscL; binding constants are greater than those for phosphatidylcholine and decrease with increasing ionic strength, suggesting that charge interactions are important in binding these anionic phospholipids. Quenching experiments suggest two classes of lipid binding sites on TbMscL for phosphatidic acid, binding of phosphatidic acid being much less dependent on ionic strength than binding of phosphatidylserine.

Intrinsic membrane proteins sit within lipid bilayers, spanning the lipid bilayer as one or more transmembrane α-helices, except in the case of bacterial outer membrane proteins, which are β-barrels. Packing of the transmembrane α-helices in membrane proteins containing more than one transmembrane α-helix will be affected by interaction with the surrounding lipid bilayer, and thus, the structures of such proteins must have coevolved with the lipid bilayer component of the membrane to give a functional membrane system. Biological membranes contain mixtures of zwitterionic and anionic lipids, and crystal structures of some membrane proteins such as bacterial photosynthetic reaction centers (*1*), cytochrome bc_1 (*2*), and KcsA (*3*) show the presence of a small number of anionic phospholipids bound to specific sites on the protein, suggesting that these sites have a high affinity for anionic phospholipids. Other anionic phospholipids will interact less specifically with the transmembrane surface of the protein, the anionic phospholipid headgroup interacting with the charged amino acid residues that often flank transmembrane α-helices. The structure of the lipid fatty acyl chains will also be important, since this defines the hydrophobic thickness of the lipid bilayer, defined as the separation between the glycerol backbone regions of the two leaflets making up the bilayer. The hydrophobic thickness of the lipid bilayer surrounding a membrane protein is likely to match the thickness of the hydrophobic, transmembrane domain of the protein because the cost of exposing hydrophobic groups on either the protein or the lipid to water is very high (*4*). The efficiency of hydrophobic matching has been confirmed in experiments with the potassium channel KcsA, which show that the Trp residues in KcsA maintain their locations close to the glycerol backbone region of the surrounding lipid bilayer as the fatty acyl chains are varied in length from C10 to C24 (*5*).

[†] We thank the BBSRC for a studentship (to A.M.P.).

* To whom correspondence should be addressed. Phone: 44 (0) 2380 594331. Fax: 44 (0) 2380 594459. E-mail: agl@soton.ac.uk.

10.1021/bi034995k CCC: $25.00
Published on Web 11/11/2003

Any potential mismatch between the hydrophobic thickness of a membrane protein and the hydrophobic mismatch of the lipid bilayer could be overcome by a distortion of the lipid bilayer around the protein, by a distortion of the membrane protein, or by some combination of both. The possibility that membrane proteins distort to help match the hydrophobic thickness of the surrounding lipid bilayer is suggested by the fact that the membrane proteins such as Ca^{2+}-ATPase (*6*−*8*), Na^+,K^+-ATPase (*9*), diacylglycerol kinase (*10*), rhodopsin (*11*), and the glucose transporter of red blood cells (*12*) all show highest activities in bilayers of phospholipids with a particular fatty acyl chain length, generally C18, activities decreasing as the chain length increases or decreases from this optimal value. The most likely distortions of an α-helical membrane protein in response to a change in bilayer thickness are a change in the tilt angle of the transmembrane α-helices, a change in the tilt angle between the long axis of the helix and the normal to the bilayer surface, changing the effective transmembrane thickness of the protein, or rotation of side chains at the ends of the helices about the Cα−Cβ bonds linking the side chains to the polypeptide backbone.

The alternative possibility, that the lipid bilayer distorts around a rigid membrane protein to achieve hydrophobic matching, has been approached theoretically (*13*−*15*). In these models, if the hydrophobic thickness of the lipid bilayer is less than that of the protein, then the fatty acyl chains will stretch to provide matching. If, on the other hand, the hydrophobic thickness of the bilayer is greater than that of the protein, then the fatty acyl chains will compress to provide matching. Either stretching or compressing the fatty acyl chains of the lipid requires work, so a lipid molecule that has to change its hydrophobic thickness to bind to a membrane protein would be expected to bind less strongly to the protein than a lipid for which no stretching or compressing is required. Thus, the possibility that hydrophobic matching between a membrane protein and the surrounding lipid bilayer is achieved by distortion of the lipid bilayer can be tested by measuring lipid binding constants as a function of lipid fatty acyl chain length. Lipid binding constants have been obtained for a variety of membrane proteins from measurements of the quenching of the fluorescence of Trp residues in the protein by lipids containing spin-labeled or brominated fatty acyl chains (*5*−*7*, *16*−*18*). Because the time for two lipid molecules to exchange between the bulk lipid phase and the annular shell of lipids around a membrane protein is greater than the fluorescence lifetime (*16*, *19*), the level of fluorescence quenching observed in a mixture of a normal lipid and a quenching lipid is proportional to the fraction of annular sites occupied by the quenching lipid, and so is dependent on the binding constant of the quenching lipid.

Phospholipids containing brominated fatty acyl chains are prepared by addition of bromine across the double bond in the corresponding phospholipid containing *cis*-unsaturated fatty acyl chains. Phospholipids containing brominated fatty acyl chains behave much like conventional phospholipids with unsaturated fatty acyl chains because the bulky bromine atoms have effects on lipid packing that are similar to those of a *cis* double bond (*7*). Phospholipids in the liquid crystalline phase show close to ideal mixing (*7*, *20*) so that analysis of the quenching results will not be complicated by any phase separation of the lipid molecules within the plane of the bilayer, for lipid mixtures in the liquid crystalline phase.

A complication of the fluorescence quenching method for determining lipid binding constants is that most membrane proteins contain several Trp residues. Analysis of Trp fluorescence quenching data for membrane proteins generally requires the assumptions to be made that all the Trp residues that are quenched by the quenching lipid are quenched to the same extent, and that all the lipid binding sites close to quenched Trp residues have equal affinities for the quenching lipid. If a membrane protein contains only a single Trp residue, then it is no longer necessary to make these simplifying assumptions. Bacterial mechanosensitive ion channels of large conductance (MscL's) generally contain few Trp residues, those from *Escherichia coli* and *Mycobacterium tuberculosis*, for example, containing none (*21*). We therefore have the opportunity of introducing single Trp residues into regions of interest in the protein. Although the MscL's are homopentameric (*22*), so that the intact channel will contain five Trp residues if one Trp residue is introduced into each monomer, lipid interactions with each monomer in the pentamer will be identical so that the quenching properties of each Trp residue will also be identical. MscL from *M. tuberculosis* (TbMscL)[1] has the additional advantage that its crystal structure has been determined (*22*). Each monomer in the homopentameric structure contains just two transmembrane α-helices (Figure 1). We have chosen to replace the lipid-exposed Phe-80 toward the center of the second transmembrane α-helix of TbMscL with Trp. We have also introduced a Trp residue into MscL from *E. coli* (EcMscL) at Phe-93, equivalent to Tyr-87 or Phe-88 in TbMscL, both Tyr-87 and Phe-88 in TbMscL being lipid-exposed residues located toward the C-terminal end of the second transmembrane α-helix (Figure 1).

Here we report a procedure for the reconstitution of MscL into lipid bilayers of defined composition and report on the dependence of phospholipid binding constants on fatty acyl chain length and headgroup structure.

MATERIALS AND METHODS

Materials and General Procedures. Dimyristoleoylphosphatidylcholine [di(C14:1)PC], dipalmitoleoylphosphatidylcholine [di(C16:1)PC], dioleoylphosphatidylcholine [di(C18:1)PC], dieicosenoylphosphatidylcholine [di(C20:1)PC], dierucoylphosphatidylcholine [di(C22:1)PC], dinervonylphos-

[1] Abbreviations: EcMscL, mechanosensitive channel of *E. coli*; TbMscL, mechanosensitive channel of *M. tuberculosis*; di(C12:0)PC, didodecylphosphatidylcholine; di(C14:1)PC, dimyristoleoylphosphatidylcholine; di(C16:1)PC, dipalmitoleoylphosphatidylcholine; di(C18:1)PC, dioleoylphosphatidylcholine; di(C20:1)PC, dieicosenoylphosphatidylcholine; di(C22:1)PC, dierucoylphosphatidylcholine; di(C24:1)PC, dinervonylphosphatidylcholine; di(C18:1)PE, dioleoylphosphatidylethanolamine; di(C18:1)PA, dioleoylphosphatidic acid; di(C18:1)PS, dioleoylphosphatiodylserine; di(C18:1)PG, dioleoylphosphatidylglycerol; tetra(C18:1)CL, tetraoleoylcardiolipin; di(Br_2C14:0)PC, di(9,10-dibromomyristoyl)phosphatidylcholine; di(Br_2C16:0)PC, di(9,10-dibromopalmitoyl)phosphatidylcholine; di(Br_2C18:0)PC, di(9,10-dibromostearoyl)-phosphatidylcholine; di(Br_2C20:0)PC, di(11,12-dibromoeicosanoyl)-phosphatidylcholine; di(Br_2C22:0)PC, di(13,14-dibromodocosanoyl)-phosphatidylcholine; di(Br_2C24:0)PC, di(15,16-dibromotetracosanoyl)phosphatidylcholine; tetra(Br_2C18:0)CL, tetra(9,10-dirbomostearoyl)-cardiolipin; di(Br_2C18:0)PA, di(9,10-dibromostearoyl)phosphatidic acid; di(Br_2C18:0)PE, di(9,10-dibromostearoyl)phosphatidyethanolamine.

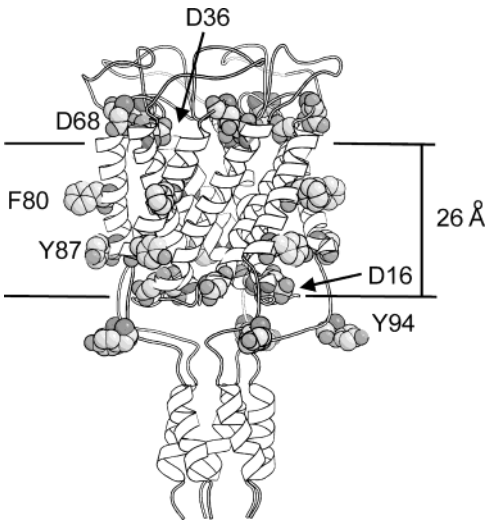

FIGURE 1: Structure of the TbMscL pentamer. The hydrophobic thickness of the protein is defined by the positions of Asp-36, Asp-68, and Asp-16, shown in space-fill format. Also shown in space-fill format are Phe-80, Tyr-87, and Tyr-94. The figure was prepared using Bobscript (*49*) and the coordinates in PDB 1MSL.

phatidylcholine [di(C24:1)PC], dioleoylphosphatidylethanolamine [di(C18:1)PE], dioleoylphosphatidic acid [di(C18:1)-PA], dioleoylphosphatiodylserine [di(C18:1)PS], dioleoylphosphatidylglycerol [di(C18:1)PG], and tetraoleoylcardiolipin [tetra(C18:1)CL] were obtained from Avanti Polar Lipids. Didodecylphosphatidylcholine [di(C12:0)PC] was obtained from Sigma. The phosphatidylcholines were brominated as described by East and Lee (*7*) to give the corresponding brominated analogues, as follows: di(9,10-dibromomyristoyl)-phosphatidylcholine [di(Br_2C14:0)PC], di(9,10-dibromopalmitoyl)phosphatidylcholine [di(Br_2C16:0)PC], di(9,10-dibromostearoyl)phosphatidylcholine [di(Br_2C18:0)PC], di(11,12-dibromoeicosanoyl)phosphatidylcholine [di(Br_2C20:0)PC], di(13,14-dibromodocosanoyl)phosphatidylcholine [di(Br_2C22:0)PC], di(15,16-dibromotetracosanoyl)phosphatidylcholine [di(Br_2C24:0)PC]. Similarly, di(C18:1)PE, di(C18:1)PA, di(C18:1)PS, di(C18:1)PG, and tetra(C18:1)CL were brominated to give the corresponding phospholipids containing 9,10-dibromostearoyl chains.

Mutagenesis and Purification of MscL. Plasmids containing the *E. coli* and *M. tuberculosis MscL* genes with poly-His epitopes at the N-termini were the generous gifts of Professors B. Martinac and D. C. Rees, respectively. Site-directed mutagenesis was performed using the Quick-change protocol from Stratagene. Mutated MscL's were prepared with a Phe residue substituted by Trp at position 80 (F80W) in TbMscL and at position 93 (F93W) in EcMscL. F80W-TbMscL was produced using synthetic oligonucleotide primers 5′-GCAGCGATCAACTTTT*GG*CTAATTGCGTTT-GCGGTGTACTTCC-3′ and 5′-GGAAGTACACCGCAAA-CGCAATTAG*CC*AAAAGTTGATCGCTGC-3′; the mutations are italic. F93W-EcMscL was produced using synthetic oligonucleotide primers 5′-GTGGCCTTTGCGATCT*G-G*ATGGCGATTAAGCTAATC-3′ and 5′-GATTAGCT-TAATCGCCAT*CC*AGATCGCAAAGGCCAC-3′. Following PCR mutagenesis, the native methylated DNA templates were digested with *Dpn*I (Promega) for 2 h at 37 °C. The mutations were confirmed by DNA sequencing.

E. coli BL21(DE3)pLysS transformants carrying the pET-19b plasmid (Novagen) with the *TbMscL* gene or *E. coli* M15[pREP4] carrying the pQE-32 plasmid (Qiagen) with the *EcMscL* gene were grown in 6 L of Luria broth to mid log phase (OD_{600} = 0.6) and then induced for 4 h in the presence of isopropyl β-D-thiogalactopyranoside (1.0 mM). MscL was purified using a protocol modified from that described by Williamson et al. (*5*). The cells were washed, resuspended in PBS buffer (60 mL; 140 mM NaCl, 2.7 mM KCl, 10 mM Na_2HPO_4, 1.8 mM KH_2PO_4, pH 7.2), and lysed by sonication. The sample was spun at 100000*g* for 40 min, and the membrane pellet was solubilized in 120 mL of PBS containing 40 mM *n*-octyl β-D-glucopyranoside (octyl glucoside; Bachem) at 4 °C for 4 h. The sample was spun at 8000*g* for 20 min and the supernatant applied to a 10 mL Ni-NTA column (Qiagen). The column was washed with PBS (6 times the agarose bed volume) containing 40 mM octyl glucoside and 30 mM imidazole; the eluate was monitored at 280 nm to ensure the removal of all nonbound protein. MscL was eluted with PBS containing 40 mM octyl glucoside and 400 mM imidazole and stored at −80 °C until use. The homogeneity of MscL was assessed by sodium dodecyl sulfate−polyacrylamide gel electrophoresis (SDS−PAGE), using the method of Laemmli (*23*).

Reconstitution of MscL. Purified MscL was reconstituted into lipid bilayers by mixing lipid and MscL in cholate, followed by dilution into buffer to decrease the concentration of cholate below its critical micelle concentration, as described for KcsA (*5*). For reconstitution into bilayers of a single phospholipid, the required phospholipid (0.47 μmol) was dried from a chloroform solution onto the walls of a thin glass vial. Buffer (400 μL; 20 mM Hepes, 100 mM KCl, 1 mM EGTA, pH 7.2) containing 15 mM cholate was added, and the sample was sonicated to clarity in a bath sonicator (Ultrawave). MscL (80 μg) was then added and the suspension incubated at 25 °C for 15 min before use. For reconstitution into bilayers containing a mixture of two lipids, separate solutions of the two lipids were prepared in cholate-containing buffer as described above. These were then mixed in the appropriate proportions, incubated at 35 °C for 30 min, and then mixed with MscL, as described above.

Gradient centrifugation was used to characterize the reconstituted preparation. Di(C18:1)PE was labeled with rhodamine isothiocyanate as described (*24*). Di(C18:1)PC (1.8 μmol) was mixed with rhodamine-labeled di(C18:1)PE (94 nmol) in chloroform, and the mixture was dried onto the walls of a glass vial. The mixture was resuspended in buffer (1.6 mL; 20 mM Hepes, 100 mM KCl, 1 mM EGTA, pH 7.2) containing 15 mM cholate. The sample was sonicated to clarity in a sonication bath (Ultrawave). EcMscL (0.32 mg) was added and the mixture incubated at 25 °C for 15 min. The sample was then dialyzed at 4 °C against two lots of buffer (500 mL; 20 mM Hepes, 100 mM KCl, 1 mM EGTA, pH 7.2) for a total of 10 h. Samples of dialysate (1.5 mL) were loaded onto sucrose gradients containing the following solutions of sucrose (w/w) in the above buffer: 2.5%, 5.0%, 10.0%, 15.0%, 20.0%, and 30.0%; the 30% sucrose solution also contained 0.05% (w/v) Triton X-100. Samples were spun at 80000*g* for 18 h at 4 °C, and then 1.5 mL fractions were collected from the gradients and analyzed for lipid and protein by, respectively, absorbance at 570 nm and Bradford protein assay.

Cross-Linking. MscL was cross-linked with disuccinimidyl suberate (DSS; Pierce). MscL (0.34 mg) was mixed with 2

μmol of lipid in cholate buffer, and the mixture was incubated at 25 °C for 15 min. The sample was then dialyzed at 4 °C against two lots of buffer (500 mL; 20 mM Hepes, 100 mM KCl, pH 7.2) for 10 h using dialysis tubing with a molecular weight cutoff of 7000. Aliquots of dialysate (100 μL) were cross-linked in the presence of DSS (2.18 mM) for 30 min at room temperature. Tris (83 mM) was added and the mixture incubated at room temperature for a further 15 min to quench the reaction. MscL (14 μg) was subsequently resolved by 10% SDS−PAGE using the method of Laemmli (*23*) and the protein visualized by staining with Coomassie Brilliant Blue.

Phospholipid Analysis. Phospholipids were extracted from purified EcMscL and TbMscL with chloroform/methanol/water at a final ratio (v/v) of 2:1:1 using the method of Bligh and Dyer (*25*). The phospholipid content was determined by phosphate analysis using the method of Bartlett (*26*).

Fluorescence Measurements and Analysis. For fluorescence measurements 250 μL of the sample was diluted into 2.75 mL of buffer (20 mM Hepes, 100 mM KCl, 1 mM EGTA, pH 7.2) and the fluorescence recorded on an SLM 8100 fluorimeter with excitation at 280 nm.

Quenching of Trp fluorescence by brominated phospholipids was fitted to a lattice model for quenching (*6*, *16*, *17*, *27*). The probability that any particular Trp residue will give rise to fluorescence is proportional to the probability that none of the *n* lattice sites close enough to the residue to cause quenching are occupied by a brominated lipid so that

$$F = F_{min} + (F_o - F_{min})(1 - x_{Br})^n \quad (1)$$

where F_o and F_{min} are the fluorescence intensities for MscL in nonbrominated and brominated lipids, respectively, and F is the fluorescence intensity in the phospholipid mixture when the mole fraction of brominated lipid is x_{Br}. This can be extended to the case where the brominated and nonbrominated lipids have different affinities for MscL. The fraction of sites f_{Br} occupied by brominated lipid is given by

$$f_{Br} = Kx_{Br}/(Kx_{Br} + [1 - x_{Br}]) \quad (2)$$

where K is the binding constant of the brominated lipid relative to that of the nonbrominated lipid. Fluorescence quenching then fits the equation

$$F = F_{min} + (F_o - F_{min})(1 - f_{Br})^n \quad (3)$$

Equations 1 and 3 were fitted to the experimental data using the nonlinear least-squares routine in the SigmaPlot package.

In Vivo Cell Viability Assay. E. coli MJF465 transformants (*28*) carrying the pET-19b plasmid with the *TbMscL* gene or the pQE-32 plasmid with the *EcMscL* gene were grown in 10 mL of Luira broth containing ampicillin (100 μg/mL) and supplemented with 0.5 M NaCl. Cells were grown in the presence of isopropyl β-D-thiogalactopyranoside (1.0 mM) for 16 h at 37 °C. Overnight cultures (200 μL) were used to seed fresh cultures (10 mL) in the same medium and grown to mid exponential phase ($OD_{600} = 0.5$). The cells were harvested by centrifugation at 3000 rpm in a benchtop centrifuge for 10 min. The culture supernatant was removed and the cell pellet resuspended in 0.5 M NaCl (1 mL). The cultures (30 μL) were diluted 50-fold into six shock solutions of various osmotic strengths between 0.5 and 0 M NaCl, containing ethidium bromide (0.5 μg/mL). The cells were incubated in the dark for 45 min at room temperature followed by centrifugation at 14000 rpm for 10 min. The supernatant was assayed for release of DNA by measuring the fluorescence intensity at 25 °C using an SLM 8100 fluorimeter with excitation and emission wavelengths of 254 and 632 nm, respectively. Results were corrected for background light scatter.

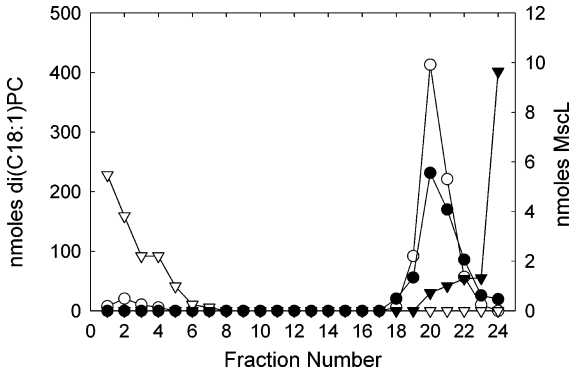

FIGURE 2: Sucrose gradient analysis of the reconstituted EcMscL. A sample of MscL reconstituted with di(C18:1)PC at a lipid:protein molar ratio of 100:1 was separated on a discontinuous sucrose gradient from 30% to 2.5% sucrose. Fractions of 1.5 mL were taken and analyzed for lipid (○) and MscL (●). Lipid alone (▽) and MscL alone (▼) were also analyzed employing the same gradient.

RESULTS

Phospholipid Content of Purified MscL. EcMscL and TbMscL purified using octyl glucoside as detergent were analyzed for phospholipid content, but no phospholipid could be detected. Similarly, no phospholipids could be detected using thin-layer chromatography.

Reconstitution of MscL. EcMscL and TbMscL were reconstituted into bilayers of defined composition by mixing the purified protein with phospholipid in cholate as detergent to give a 100:1 molar ratio of phospholipid to MscL monomer, followed by 12-fold dilution into buffer to drop the concentration of cholate below its critical micelle concentration, thus re-forming membranes, as used for the reconstitution of Ca^{2+}-ATPase, KcsA, and diacylglycerol kinase (*5*, *7*, *10*). This procedure gives large, unsealed membrane fragments. Full reconstitution of MscL into lipid bilayers under these conditions was confirmed in a number of ways. Reconstituted EcMscL was characterized by centrifugation on a discontinuous sucrose gradient (Figure 2). When EcMscL and lipid are run separately on the gradient, all the EcMscL is found at the bottom of the gradient and all of the lipid is found at the top of the gradient. However, when EcMscL is reconstituted with di(C18:1)PC, EcMscL is found at the 20−30% sucrose interface along with the lipid (Figure 2). The molar ratio of lipid to protein in the EcMscL-containing fraction is about 60:1, compared to 100:1 in the original mixture. The calculated density of the reconstituted sample was 1.114 g cm^{-3}, consistent with its location at the 20−30% sucrose interface (densities of 1.081 and 1.127 g cm^{-3}, respectively), showing that EcMscL has reconstituted with the phospholipid.

Reconstitution was also confirmed using fluorescence spectroscopy. The fluorescence emission spectrum of F80W-

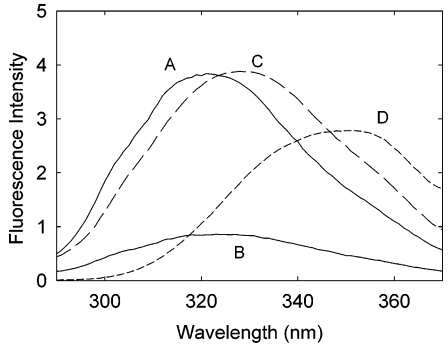

FIGURE 3: Fluorescence emission spectra for F80W-TbMscL and F93W-EcMscL. Fluorescence emission spectra are shown for F80W-TbMscL (A) and F93W-EcMscL (C) reconstituted into bilayers of di(C18:1)PC, and F80W-TbMscL reconstituted into bilayers of di(Br_2C18:0)PC (B). The concentration of MscL was 0.98 μM at a molar ratio of lipid to MscL of 100:1. The emission spectrum of 0.98 μM Trp in buffer (D) is also shown. The buffer was 20 mM Hepes, 100 mM KCl, 1 mM EGTA, pH 7.2.

Table 1: Effect of the Method of Reconstitution on Fluorescence Quenching of F80W-TbMscL by Di(Br_2C18:0)PC[a]

method	F/F_o
15 mM cholate/12-fold dilution	0.18 ± 0.02
15 mM cholate/60-fold dilution	0.19 ± 0.04
30 mM cholate/12-fold dilution	0.17 ± 0.02
30 mM cholate/60-fold dilution	0.18 ± 0.03
15 mM cholate/dialysis	0.20 ± 0.01

[a] F and F_o are fluorescence intensities for TbMscL reconstituted in di(Br_2C18:0)PC and di(C18:1)PC, respectively. Fluorescence was excited at 280 nm, and emission was monitored at 322 nm.

TbMscL reconstituted into bilayers of di(C18:1)PC by mixing in 15 mM cholate followed by a 12-fold dilution to re-form membranes is shown in Figure 3. The emission spectrum is centered at 322 nm, indicating a very hydrophobic environment for the Trp residue. The fluorescence emission maximum for F93W-EcMscL is at 328 nm (Figure 3), shifted slightly to longer wavelengths compared to that of F80W-TbMscL. Reconstitution of F80W-TbMscL into bilayers of di(Br_2C18:0)PC led to quenching of 82% of the Trp fluorescence of TbMscL (Figure 3, Table 1). Increasing the dilution factor used to re-form membranes 60-fold had no significant effect on the level of fluorescence quenching, and increasing the cholate concentration to 30 mM also had no significant effect (Table 1). The level of fluorescence quenching observed using dialysis to remove detergent was the same as that observed using the dilution method (Table 1).

MscL crystallizes as a pentamer, and cross-linking MscL in the native membrane results in a ladder-like pattern on SDS gels, corresponding to multiples of the monomeric protein up to a pentamer or higher (*29*, *30*). SDS gels of EcMscL and TbMscL before cross-linking show the presence of predominantly monomeric species, with small amounts of dimer (Figure 4), as previously reported by Chang et al. (*22*). Cross-linking EcMscL or TbMscL reconstituted in di(C18:1)PC results in a ladder-like pattern of bands extending up to the pentameric species (Figure 4), consistent with MscL retaining its pentameric structure after reconstitution. Reconstitution of TbMscL in short- or long-chain phosphatidylcholines or in di(C18:1)PS or di(C18:1)PA also results in a cross-linking pattern consistent with formation of a pentamer (Figure 4).

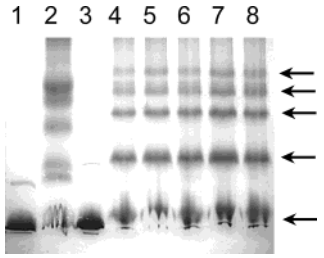

FIGURE 4: Sodium dodecyl sulfate−polyacrylamide gel electrophoresis of MscL after cross-linking with DSS (2.18 mM) for 30 min at room temperature. Protein was visualized by staining with Coomassie Brilliant Blue. Lanes 1 and 3 contain EcMscL and TbMscL, respectively, before cross-linking. Bands correspond largely to monomeric protein (M_r of 15000 and 17000 for EcMscL and TbMscL, respectively) with small amounts of dimer. Lane 2 contains EcMscL cross-linked after reconstitution in di(C18:1)PC. Lanes 4−8 contain TbMscL cross-linked after reconstitution in di(C14:1)PC, di(C18:1)PC, di(C24:1)PC, di(C18:1)PS, and di(C18:1)PA, respectively. The arrows show the expected positions of monomeric MscL and of dimeric, trimeric, tetrameric, and pentameric species. In the reconstituted systems the molar ratio of phospholipid to MscL was 100:1.

Table 2: Fluorescence Quenching of F80W-TbMscL and F93W-EcMscL in Brominated Phospholipids as a Function of Fatty Acyl Chain Length[a]

fatty acyl chain	position of the *cis* double bond	F80W-TbMscL		F93W-EcMscL	
		F/F_o	n	F/F_o	n
C14:1	9	0.14 ± 0.01	2.67 ± 0.13	0.24 ± 0.01	1.31 ± 0.06
C16:1	9	0.15 ± 0.01	2.44 ± 0.06	0.26 ± 0.02	1.22 ± 0.07
C18:1	9	0.19 ± 0.01	2.46 ± 0.05	0.34 ± 0.01	1.35 ± 0.02
C20:1	11	0.24 ± 0.02	2.54 ± 0.21	0.43 ± 0.01	1.28 ± 0.07
C22:1	13	0.31 ± 0.02	2.64 ± 0.27	0.51 ± 0.01	1.44 ± 0.09
C24:1	15	0.41 ± 0.01	2.47 ± 0.21	0.61 ± 0.01	1.39 ± 0.03

[a] F_o and F are fluorescence intensities for MscL reconstituted in nonbrominated phospholipid and the corresponding brominated phospholipid, respectively, measured at pH 7.2. The value of n is the value obtained by fitting the data in Figure 5 to eq 1.

Fluorescence Quenching by Brominated Phospholipids. Fluorescence quenching of F80W-TbMscL in mixtures of a brominated phospholipid and the corresponding nonbrominated phospholipid fit eq 1 with the parameters listed in Table 2 (Figure 5). Values of n are identical within experimental error for all the phospholipids with an average value of 2.54. For F93W-EcMscL the values of n were again the same for all the phospholipids but with an average value of 1.33 (Figure 5, Table 2). The maximum levels of quenching of F80W-TbMscL and F93W-EcMscL decrease with increasing chain length (Figure 5, Table 2). The level of fluorescence quenching of F80W-TbMscL observed in brominated phosphatidylethanolamine is the same as that seen with brominated phosphatidylcholine (Figure 6, Table 3), but the level of quenching observed with brominated anionic phospholipids is slightly greater (Figure 6, Table 3). The values of n for all the lipid headgroups are very similar, except for phosphatidic acid and for cardiolipin. The value of n is significantly greater for di(C18:1)PA than for di(C18:1)PS or di(C18:1)PG, possibly because of the small size of the phosphatidic acid headgroup (*31*). The value for n for tetra-(C18:1)CL is about half that for di(C18:1)PS, consistent with the four-chain structure of cardiolipin compared to the two-chain structure of the other phospholipids. Values of n for quenching of F93W-EcMscL by phosphatidylethanolamine

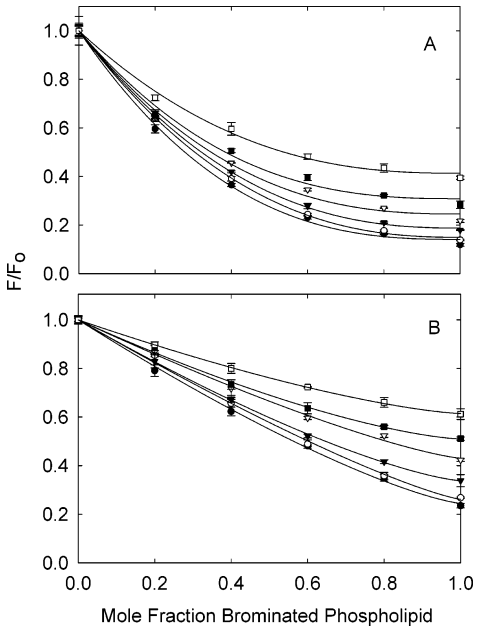

FIGURE 5: Quenching of F80W-TbMcsL and F93W-EcMscL fluorescence by brominated phosphatidylcholines. F80W-TbMscL (A) and F93W-EcMscL (B) were reconstituted into bilayers containing mixtures of nonbrominated lipid and the corresponding brominated lipid. Fluorescence intensities are expressed as a fraction of the fluorescence for MscL reconstituted in the nonbrominatd lipid. Chain lengths were as follows: (●) C14, (○) C16, (▼) C18, (▽) C20, (■) C22, (□) C24. The solid lines show fits to eq 1 giving the values for *n* listed in Table 2. The concentration of MscL was 0.98 μM, and the molar ratio of lipid to MscL was 100:1.

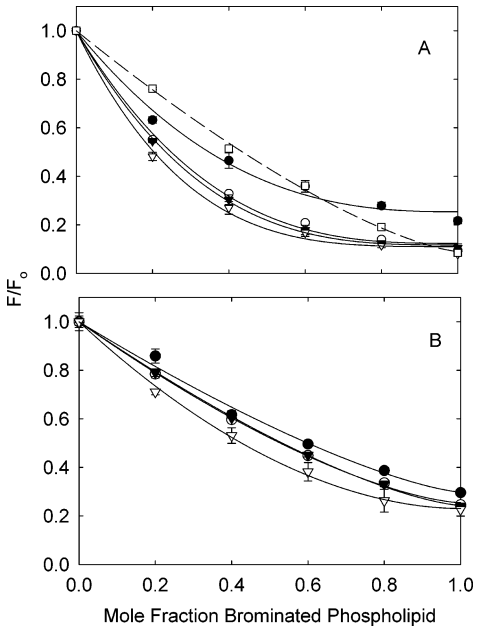

FIGURE 6: Quenching of fluorescence by brominated phospholipids. F80W-TbMscL (A) and F93W-EcMscL (B) were reconstituted into bilayers containing mixtures of nonbrominated lipid and the corresponding brominated lipid, all the lipids having C18 chains. Fluorescence intensities are expressed as a fraction of the fluorescence for MscL reconstituted in the nonbrominatd lipid. Lipid headgroups were as follows: (●) di(C18:1)PE, (○) di(C18:1)PS, (▼) di(C18:1)PG, (▽) di(C18:1)PA, (□) tetra(C18:1)CL. The lines show fits to eq 1 giving the values for *n* listed in Table 3. The concentration of MscL was 0.98 μM, and the molar ratio of lipid to MscL was 100:1.

and by anionic phospholipids are similar to those for phosphatidylcholine, except for phosphatidic acid, for which the value of *n* is again greater than for the other phospholipids (Table 3).

Table 3: Fluorescence Quenching of F80W-TbMscL and F93W-EcMscL in Brominated Phospholipids as a Function of Lipid Headgroup[a]

	F80W-TbMscL		F93W-EcMscL	
phospholipid	F/F_o	n	F/F_o	n
di(C18:1)PE	0.25 ± 0.02	2.59 ± 0.29	0.30 ± 0.02	1.36 ± 0.13
di(C18:1)PS	0.12 ± 0.01	2.95 ± 0.22	0.25 ± 0.01	1.48 ± 0.04
di(C18:1)PG	0.12 ± 0.01	3.12 ± 0.10	0.24 ± 0.01	1.42 ± 0.03
di(C18:1)PA	0.11 ± 0.01	3.62 ± 0.27	0.23 ± 0.01	1.89 ± 0.09
tetra(C18:1)CL	0.09 ± 0.01	1.39 ± 0.05		

[a] F_o and F are fluorescence intensities for MscL reconstituted in nonbrominated phospholipid and the corresponding brominated phospholipid, respectively, measured at pH 7.2. The value of *n* is the value obtained by fitting the data in Figure 6 to eq 1.

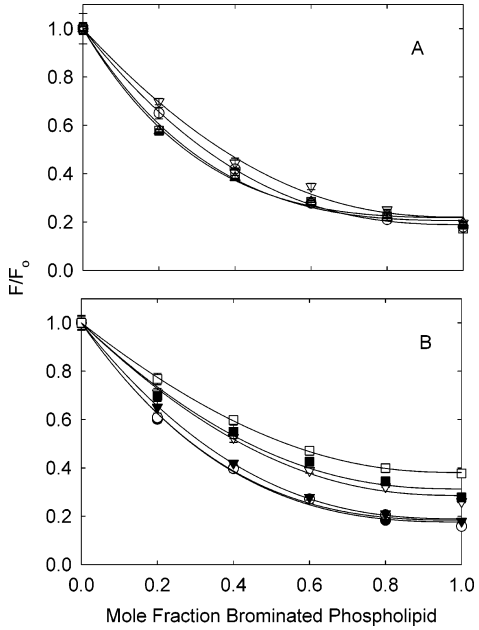

FIGURE 7: Quenching of F80W-TbMscL in mixtures with brominated phosphatidylcholines. (A) F80W-TbMscL was reconstituted into mixtures of di(Br_2C18:0)PC and (□) di(C12:0)PC, (▽) di(C16:1)PC, (○) di(C18:1)PC, and (△) di(C24:1)PC. (B). F80W-TbMscL was reconstituted into mixtures of di(C18:1)PC and (●) di(Br_2-C14:0)PC, (○) di(Br_2C16:0)PC, (▼) di(Br_2C18:0)PC, (▽) di(Br_2-C20:0)PC, (□) di(Br_2C22:0)PC, and (△) di(Br_2C24:0)PC. The solid lines show best fits to eq 3 giving the relative binding constants listed in Table 4.

Relative Lipid Binding Constants for MscL. Fluorescence quenching curves for F80W-TbMscL in mixtures of di(Br_2-C18:0)PC and phosphatidycholines of chain lengths C12, C16, C18, and C24 are shown in Figure 7A. Fluorescence quenching is slightly more marked in mixtures of di(C12:0)PC and di(Br_2C18:0)PC at intermediate mole fractions of di(Br_2C18:0)PC than in mixtures of di(C18:1)PC and di(Br_2-C18:0)PC (Figure 7A). This shows that di(C12:0)PC binds to TbMscL with a binding constant slightly smaller than that for di(C18:1)PC. In contrast, quenching in mixtures of di(C16:1)PC and di(Br_2C18:0)PC is slightly less at intermediate mole fractions of di(Br_2C18:0)PC than in mixtures of di(C18:1)PC and di(Br_2C18:0)PC, showing that di(C16:1)PC binds slightly more strongly to TbMscL than does di(C18:1)PC. Quenching profiles for other chain length lipids were intermediate between those shown in Figure 7A. Data were

Table 4: Relative Lipid Binding Constants for F80W-TbMscL and F93W-EcMscL for Phosphatidylcholines[a]

fatty acyl chain	rel binding constant measured using di(Br_2C18:0)PC	rel binding constant measured using di(C18:1)PC
	TbMscL	
C12:0	0.78 ± 0.08	
C14:1	1.05 ± 0.10	1.08 ± 0.08
C16:1	1.13 ± 0.11	1.09 ± 0.08
C18:1	1	1
C20:1	0.85 ± 0.07	0.83 ± 0.06
C22:1	0.79 ± 0.08	0.84 ± 0.11
C24:1	0.72 ± 0.05	0.78 ± 0.02
	EcMscL	
C12:0	0.73 ± 0.02	
C14:1	1.06 ± 0.05	1.13 ± 0.04
C16:1	1.13 ± 0.06	1.35 ± 0.06
C18:1	1	1
C20:1	0.61 ± 0.04	0.83 ± 0.08
C22:1	0.53 ± 0.03	0.70 ± 0.06
C24:1	0.46 ± 0.03	0.65 ± 0.08

[a] Binding constants relative to that for di(C18:1)PC were calculated from quenching data for F80W-TbMscL and F93W-EcMscL in mixtures of di(Br_2C18:0)PC with nonbrominated lipid or di(C18:1)PC with brominated lipid, at pH 7.2, using values for *n* from Table 2.

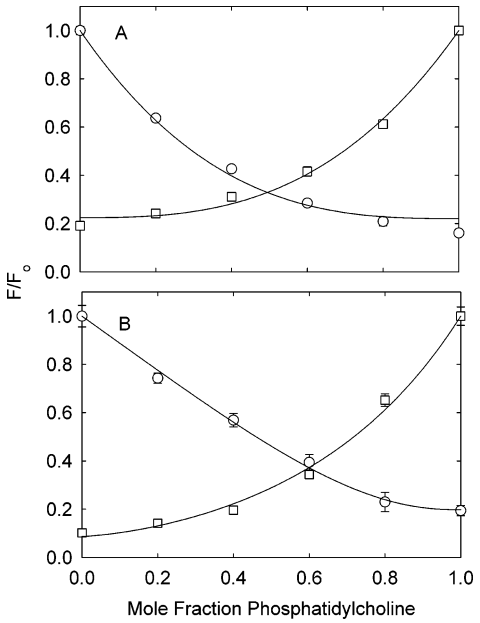

FIGURE 8: Quenching of F80W-TbMscL in mixtures with phosphatidylethanolamine (A) or cardiolipin (B). F80W-TbMscL was reconstituted into mixtures containing di(C18:1)PC and di(Br_2C18:0)PE or tetra(Br_2C18:0)CL (□) or di(Br_2C18:0)PC and di(C18:1)PE or tetra(C18:1)CL (○). The solid lines show best fits to eq 3 giving the relative binding constants listed in Table 5. In (B), mole fractions are calculated on the basis of the number of moles of fatty acyl chains to account for the fact that tetra(C18:1)CL contains four chains and di(C18:1)PC contains two chains.

analyzed in terms of eq 3 with a value for *n* of 2.54, giving the relative binding constants listed in Table 4.

Fluorescence quenching curves were also determined for the reverse experiment in which F80W-TbMscL was reconstituted in mixtures of di(C18:1)PC with brominated phospholipids with chain lengths between C14 and C24 (Figure 7B). The data were again analyzed using eq 3, giving the relative binding constants listed in Table 4. The close agreement between the two determinations of relative binding constant gives confidence in the analysis. A corresponding

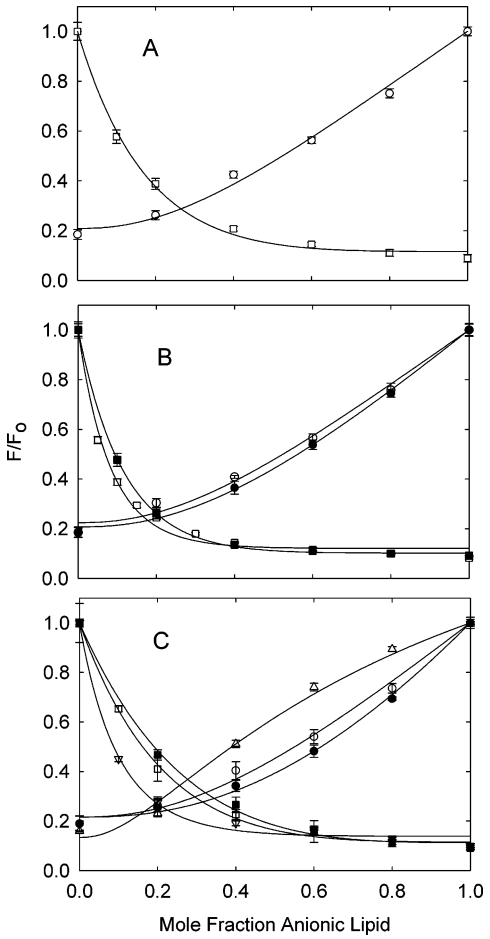

FIGURE 9: Quenching of F80W-TbMscL in mixtures of anionic lipid and phosphatidylcholine. F80W-TbMscL was reconstituted into mixtures containing di(C18:1)PC and brominated anionic phospholipid (□, ■, ▽), or nonbrominated anionic phospholipid and di(Br_2C18:0)PC (○, ●, △): (A) phosphatidylglycerol, (B) phosphatidic acid, (C) phosphatidylserine. The concentration of KCl was (▽, △) 26 mM, (□, ○) 100 mM, and (■, ●) 1 M. The solid lines show best fits to eq 3 giving the relative binding constants listed in Table 5.

analysis was performed for F93W-EcMscL (data not shown), giving the binding constants listed in Table 4.

Fluorescence quenching curves for F80W-TbMscL in mixtures of phosphatidylcholine and phosphatidylethanolamine or anionic phospholipid are shown in Figures 8 and 9. The binding constant for di(C18:1)PE relative to di(C18:1)PC is close to 1 (Figure 8, Table 5). Binding constants for phosphatidylglycerol and phosphatidylserine obtained from experiments with di(C18:1)PC and brominated anionic lipid or from experiments with di(Br_2C18:0)PC and nonbrominated anionic phospholipid are the same (Figure 9, Table 5), consistent with simple competition between phosphatidylcholines and phosphatidylglycerol or phosphatidylserine for binding to MscL. Similarly, binding constants obtained for cardiolipin from experiments with mixtures of di(C18:1)PC and tetra(Br_2C18:0)CL or di(Br_2C18:0)PC and tetra(C18:1)CL are the same, when concentrations are expressed in terms of fatty acyl chains (Figure 8, Table 5). However, for phosphatidic acid, binding constants for phosphatidic acid relative to phosphatidylcholine obtained from experiments with mixtures of di(C18:1)PC and di(Br_2-C18:0)PA do not agree with those obtained from experiments with mixtures of di(Br_2C18:0)PC and di(C18:1)PA (Figure

Table 5: Relative Lipid Binding Constants for F80W-TbMscL as a Function of Lipid Headgroup[a]

phospholipid	[KCl] (mM)	rel binding constant measured using di(Br_2C18:0)PC	rel binding constant measured using di(C18:1)PC
di(C18:1)PE	100	1.04 ± 0.07	1.14 ± 0.01
di(C18:1)PG	100	1.87 ± 0.20	1.92 ± 0.12
di(C18:1)PS	26	3.88 ± 0.40	3.57 ± 0.31
	100	2.24 ± 0.14	2.31 ± 0.19
	1000	1.26 ± 0.10	1.37 ± 0.01
di(C18:1)PA	100	1.81 ± 0.21	3.49 ± 0.25
	1000	1.62 ± 0.09	2.44 ± 0.05
tetra(C18:1)CL	100	1.96 ± 0.21	1.82 ± 0.14

[a] Binding constants relative to that for di(C18:1)PC were calculated from quenching data for F80W-TbMscL in mixtures of di(Br_2C18:0)PC with nonbrominated lipid or di(C18:1)PC with brominated lipid, at pH 7.2, using the values for n given in Table 3 for experiments with di(C18:1)PC and $n = 2.54$ for experiments with di(Br_2C18:0)PC. For tetra(C18:1)CL the mole fraction is calculated on the basis of the number of moles of fatty acyl chains to account for the fact that tetra(C18:1)CL contains four chains and di(C18:1)PC contains two chains.

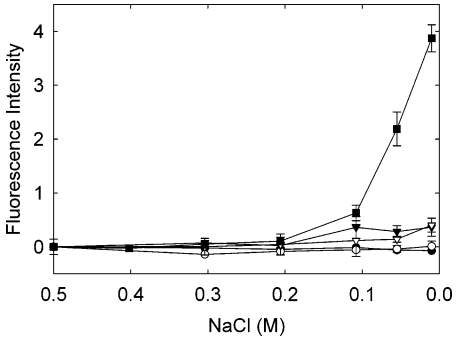

FIGURE 10: In vivo cell viability assay for the function of MscL. Cells were grown in the presence of 0.5 M NaCl to mid exponential phase as described in the text, followed by a 50-fold dilution into solutions containing the given concentrations of NaCl, supplemented with 0.5 μg/mL ethidium bromide. The samples were centrifuged, and the fluorescence emission of the supernatant was recorded at 632 nm to assay for released DNA. Key: *E. coli* strain MJF465 (■) and MJF465 expressing wild-type EcMscL (●), wild-type TbMscL (○), F93W-EcMscL (▼), and F80W-TbMscL (▽).

9, Table 5). The marked quenching observed in mixtures with di(Br_2C18:0)PA suggests that di(Br_2C18:0)PA binds strongly to TbMscL, but the experiments with di(C18:1)PA suggest that di(C18:1)PA is unable to displace di(Br_2C18:0)PC from around TbMscL with the efficiency expected from the experiments with di(Br_2C18:0)PA. Similar observations have been made previously in studies of anionic lipid binding to the potassium channel KcsA, and to simple transmembrane α-helices (*27*, *31*). The most obvious explanation for this result is that there are two classes of binding sites around MscL for phospholipid, one class of sites showing a higher affinity for phosphatidic acid than the other. Increasing ionic strength leads to a decrease in the relative affinities of both phosphatidylserine and phosphatidic acid for F80W-TbMscL (Figure 9, Table 5).

In Vivo Cell Viability Assay for the Function of MscL. An in vivo assay was used to show that the mutant McsL's were functional, using a fluorescence assay to measure levels of the release of DNA following osmotic shock. Wild-type and mutant EcMscL and TbMscL were expressed in *E. coli* strain MJF465 lacking mechanosensitive ion channels, making them sensitive to osmotic downshock (*28*). As shown in Figure 10 both the wild-type and mutant EcMscL and TbMscL are able to rescue the *E. coli* cells from the effects of osmotic downshock, confirming that introduction of the Trp residues into the channels does not inactivate the channels.

DISCUSSION

Introduction of Trp Residues into MscL. Trp fluorescence spectroscopy is a powerful technique for studying the structures of membrane proteins because of the environmental sensitivity of Trp fluorescence emission. It is also possible to use fluorescence spectroscopy to study interactions between membrane proteins and the surrounding lipid bilayer, making use of the ability of phospholipids containing spin-labeled or brominated fatty acyl chains to quench Trp fluorescence (*5*−*7*, *16*−*18*). However, analysis of fluorescence data for a membrane protein can be complicated if the protein contains a large number of Trp residues, all in different environments. An ideal membrane protein for fluorescence studies would therefore contain a single Trp residue since then, for example, fluorescence quenching studies with brominated phospholipids would provide information only about lipid interactions in the vicinity of that Trp residue. In the case where the single Trp residue is introduced by mutagenesis into a Trp-free protein, there is the additional advantage that it is possible to change the location of the Trp residue and so provide information about lipid interactions with a variety of sites on the protein, depending on the location of the Trp residue.

Here we show that this approach can be adopted to study lipid interactions with MscL. Because MscL is a homopentamer, introduction of a single Trp residue into the monomer will result in a channel containing five Trp residues. However, each monomer in the pentamer is in an identical environment so that the quenching properties of each Trp residue will also be identical. We chose to introduce the Trp residue in TbMscL at the position of Phe-80, a residue on the second transmembrane α-helix that will be exposed to the surrounding lipid bilayer, close to the middle of the bilayer (Figure 1). This would be expected to introduce the minimum perturbation into the protein, since lipid-exposed residues are generally not conserved and since Trp residues are well accommodated in the middle of a transmembrane α-helix, as shown by studies with simple model transmembrane α-helices (see ref *18*). The in vivo cell viability assay shown in Figure 10 shows that the mutant TbMscL is functional in *E. coli*. We also replaced Phe-93 in EcMscL with Trp; Phe-93 is also a lipid-exposed residue, but located toward the cytoplasmic end of the second transmembrane α-helix. The fact that the mutant EcMscL was also active in the in vivo cell viability assay (Figure 10) suggests that this mutation also does not block the function of the channel.

Reconstitution of MscL. We have shown that a variety of membrane proteins can be reconstituted by mixing with phospholipid in a suitable detergent such as cholate or octylpolyoxyethylene (octyl-POE) followed by dilution below the critical micelle concentration of the detergent to re-form membranes (*5*, *10*, *17*, *32*). Here we reconstitute TbMscL and EcMscL using the cholate dilution procedure. Reconstituted protein was characterized on a discontinuous

sucrose gradient, confirming that the protein and lipid mix in the reconstitution procedure (Figure 2). Cross-linking experiments suggest that TbMscL and EcMscL maintain their pentameric structures when reconstituted into bilayers of phosphatidylcholines with chain lengths between C14 and C24 or into bilayers of di(C18:1)PS or di(C18:1)PA (Figure 4), confirming that the reconstitution procedure does not result in denaturation of the protein.

Fluorescence Properties of F80W-TbMscL and F93W-EcMscL. We replaced Phe-80 in TbMscL and Phe-93 in EcMscL with Trp residues; Phe-93 in EcMscL is equivalent to Tyr-87 or Phe-88 in TbMscL, and Phe-80, Tyr-87, and Phe-88 in TbMscL are all lipid-exposed residues (Figure 1). The fluorescence emission spectrum for F80W-TbMscL reconstituted into di(C18:1)PC shows the Trp residue to be located in a very hydrophobic environment (Figure 3). The small shift of the emission spectrum for F93W-EcMscL to longer wavelengths (Figure 3) is consistent with a location for the Trp residue in the hydrophobic core of the bilayer, but slightly closer to the membrane interface.

The Trp fluorescences of both F80W-TbMscL and F93W-EcMscL are quenched by brominated phospholipids (Figures 3 and 5). Fluorescence quenching in mixtures of a brominated lipid with the corresponding nonbrominated lipid has been fitted to a lattice model (eq 1), where n is the number of lipid molecules close enough to the Trp residue to cause quenching (*6*, *16*, *17*, *27*). For F80W-TbMscL the value of n for the phosphatidylcholines is independent of chain length (Table 2) and has a value comparable to those observed for simple Trp-containing transmembrane α-helices, which have n values in the range from 2.3 to 2.7 (*18*). This suggests that the Trp residue in F80W-TbMscL is fully exposed to the lipid bilayer. The value of n in the four-chain lipid tetra-(diC18:1)CL is half that in the two-chain phosphatidylcholines (Table 3), consistent with n being a measure of the number of lipid molecules close to a Trp residue. Changes in n with lipid headgroup are generally small, except for phosphatidic acid, for which the n number is significantly higher than for the other phospholipids (Table 3); a similar observation has been made for quenching of the fluorescence of KcsA by brominated phospholipids and attributed to the small size of the phosphatidic acid headgroup (*31*). Values of n for F93W-EcMscL are smaller than those for F80W-TbMscL (Tables 3 and 4), with values comparable to those observed previously for quenching of the Trp fluorescence of KcsA, for which the value of n was ca. 1.69 (*5*). The smaller value for n suggests that the Trp residue in F93W-TbMscL is more buried within the protein than that in F80W-TbMscL.

The level of fluorescence quenching observed for F80W-TbMscL can be compared with the expectations of a simple model for quenching. Quenching of Trp fluorescence by dibrominated quenchers fits an equation with a sixth-power dependence on the distance of separation between the Trp residue and the quencher, as in Forster energy transfer (*33*, *34*). Bolen and Holloway (*33*) estimated a value for R_o, the distance at which energy transfer is 50% efficient, of 9.25 Å for quenching of a Trp-containing peptide by brominated phospholipids containing one dibrominated fatty acyl chain but did not take into account the fact that quenching of the Trp residue, located in the middle of the lipid bilayer, could take place from both monolayers (*35*). Refitting their data gives a value for R_o of 7.8 Å, in good agreement with the value of 8.2 Å estimated by Mall et al. (*34*) for quenching of Trp by dibromotyrosine. For energy transfer by the Forster mechanism the quencher must absorb light at the wavelengths of Trp emission (*36*). The dibrominated alkane 2,3-dibromobutane shows weak absorption at wavelengths below ca. 320 nm with, for example, an extinction coefficient of 0.4 M^{-1} cm^{-1} at 290 nm. The overlap integral J between the absorption spectrum of 2,3-dibromobutane and the emission spectrum of Trp is 2.8×10^8 M^{-1} cm^3 nm^4 for a Trp in a hydrophilic environment and 8.1×10^8 M^{-1} cm^3 nm^4 for a Trp in a hydrophobic environment, giving R_o values of 3.2 and 3.8 Å, respectively. These values are significantly less than the value of R_o determined experimentally, but it is possible that molecular motion on the fluorescence time scale will lead to a significant increase in the effective R_o value, and clearly, the assumption of point dipoles in the derivation of the Forster equation will not be valid at very short distances. It is also possible, of course, that fluorescence quenching could be by a mechanism other than Forster transfer (*37*, *38*). Indeed, Ladokhin (*48*) has shown that the data of Bolen and Holloway (*33*) can be interpreted in terms of a collisional model for quenching when account is taken of the depth distributions of the fluorophore and quencher in the membrane. Nevertheless, the observation that the experimental data fit reasonably well to an R^6 curve suggests that an analysis in these terms can be used to estimate separation distances in our experiments.

The rate of energy transfer k_T for a single donor−acceptor pair can be written as (*36*)

$$k_T = (1/\tau_D)(R_o/r)^6 \quad (4)$$

where τ_D is the decay rate of the donor, r is the distance between the donor and acceptor, and R_o is the distance between the donor and acceptor at which the efficiency of energy transfer is 50%. The efficiency E of energy transfer is given by

$$E = k_T/(k_T + \tau_D{}^{-1}) \quad (5)$$

In the presence of more than one acceptor, the rate of transfer can be written as the sum of the k_T values for all the donor−acceptor pairs (*36*). Thus, in the presence of x acceptors all at the same distance from the donor the efficiency of energy transfer becomes

$$E = xR_o{}^6/(r^6 + xR_o{}^6) \quad (6)$$

In di(Br_2C18:0)PC the efficiency of quenching of the fluorescence of F80W-TbMscL is 0.81. The value for n is ca. 2.5 (Table 3), meaning that ca. five brominated fatty acyl chains are close enough to the Trp residue in F80W-TbMscL to cause quenching. Putting $x = 5.0$ in eq 6 gives a distance r of 10.2 Å.

The hydrophobic thickness d of a lipid bilayer of a saturated phosphatidylcholine in the liquid crystalline phase is related to fatty acyl chain length by the equation

$$d = 1.75(n_C - 1) \quad (7)$$

where n_C is the number of carbon atoms in the fatty acyl chain (*39*, *40*). The thickness of a bilayer of a phospha-

tidylcholine with two monounsaturated chains was estimated by Lewis and Engelman (*39*) to be about 2.5 Å less than that of the corresponding phosphatidylcholine with two saturated chains calculated from eq 7. The bromine atoms in di(Br_2C18:0)PC are at the C9 and C10 positions, which can be estimated from eq 7 to be about 6.4 Å from the bilayer center. If it is assumed that the Trp residue in F80W-TbMscL is located at the bilayer center, then the distance r between the Trp residue and the bromine atoms will be given by $(a^2 + 6.4^2)^{0.5}$, where a is the distance between the Trp residues and the bromine atoms along the bilayer surface. With $r =$ 10.2 Å, a becomes 8.0 Å. Bolen and Holloway (*33*) estimated that the combined radius of an indole−bromine pair was 7 Å. Thus, the estimated value of a is consistent with the proposal that quenching of the Trp fluorescence of F80W-TbMscL arises from the 2.5 lipid molecules in the annular shell of lipid molecules surrounding TbMscL that are closest to the Trp residue. It is also possible to calculate the expected efficiency of energy transfer to lipid molecules in the second shell around TbMscL. Assuming a diameter of 9.4 Å for a lipid molecule, the distance r becomes 18.5 Å for the closest lipid molecules in the second shell, giving a value for E of 0.03, assuming again that five chains are close enough to the Trp residue to result in quenching. Thus, the assumption that quenching arises predominantly from the annular shell of lipids around the protein is valid.

Effects of Fatty Acyl Chain Length. Binding constants for phosphatidylcholines for both F80W-TbMscL and F93W-EcMscL vary by only a factor of ca. 1.5 over the chain length range from C12 to C24 (Table 4). The phosphatidylcholine binding most strongly to F80W-TbMscL and F93W-EcMscL is di(C16:1)PC, and the hydrophobic thickness of a bilayer of di(C16:1)PC, estimated from eq 7, is about 24 Å. The crystal structure of TbMscL (*22*) does not include any resolved lipid molecules, and thus, it cannot be said for certain where the lipid bilayer is located around the protein. For many membrane proteins the probable location of the lipid bilayer around the protein can be deduced from the location of Trp and Tyr residues in the protein because Trp and Tyr residues are often found at the ends of transmembrane α-helices of membrane proteins, where they have been suggested to act as "floats" at the interface between the hydrocarbon core of the bilayer and surrounding medium, serving to fix the helix within the lipid bilayer (*41*, *42*). However, TbMscL contains no Trp residues and only two Tyr residues per monomer (Tyr-87 and Tyr-94), both on the same side of the membrane (Figure 1). The ends of transmembrane α-helices can also be marked by the presence of unpaired charged residues; the high cost of burying a charged residue within the hydrocarbon core of the bilayer makes it unlikely that unpaired charged residues will be buried within the hydrocarbon core. For TbMscL, Asp-36 and Asp-68 are likely to define the hydrocarbon core−water interface on the periplasmic side of the membrane, and if the interface on the cytoplasmic surface is defined by the position of Asp-16, then the thickness would be 26 Å (Figure 1). Asp-16 and Asp-36 are conserved in most MscL's, and although Asp-68 is not conserved, the position is generally occupied by a charged residue and is usually followed by a Tyr or Trp residue. A hydrophobic thickness of 26 Å is consistent with the observation that the phosphatidylcholine binding with highest affinity to TbMscL is di(C16:1)PC. The native *M. tuberculosis* membrane will have a hydrophobic thickness close to 24 Å since the predominant phospholipids of *M. tuberculosis* contain C18:1 and C16:0 chains at the *sn*-1 and *sn*-2 positions, respectively (*43*).

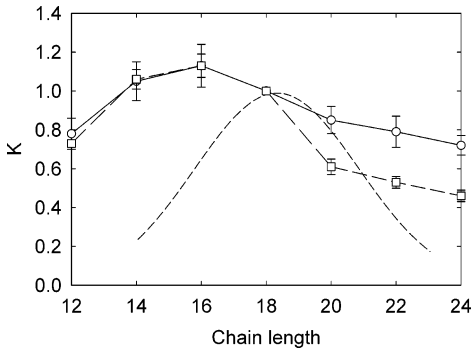

FIGURE 11: Dependence of lipid binding constants on chain length. The chain length dependencies of the binding constants for phosphatidylcholines relative to di(C18:1)PC are plotted for F80W-TbMscL (○, solid line) and F93W-EcMscL (□, long-dashed line). The short-dashed line shows the dependence of the lipid binding constant on chain length calculated from the data of Fattal and Ben-Shaul (*14*) for a protein with a hydrophobic thickness of 30 Å, as described in the text.

In bilayers containing shorter or longer chains than C16 there will be a mismatch between MscL and the lipid bilayer that would be expected to result in distortion of the lipid bilayer or the protein or both, to avoid exposure of hydrophobic groups to water. Most models of hydrophobic mismatch assume that the lipid chains in the vicinity of the protein adjust their length to the hydrophobic thickness of the protein, with the protein acting as a rigid body (*13*−*15*). When the thickness of the bilayer is less than the hydrophobic length of the protein, the lipid chains must be stretched. Conversely, when the thickness of the bilayer is greater than the hydrophobic length of the protein, the lipid chains must be compressed. Fattal and Ben-Shaul (*14*) have estimated the membrane deformation energy due to inclusion in the bilayer of a rigid protein with a 30 Å long hydrophobic domain, over the range of bilayer hydrophobic thicknesses from 40 to 20 Å. For a protein of radius 21.5 Å, the estimated radius of MscL, the deformation energies calculated using the equations of Fattal and Ben-Shaul (*14*) fit the following quadratic:

$$\Delta G = 1275 - 86.18x + 1.457x^2 \qquad (8)$$

where ΔG is the membrane deformation energy (kJ mol^{-1}) and x is the membrane thickness (Å). The circumference of MscL is about 135 Å, and with a diameter of a lipid molecule of 9.4 Å, ca. 29 lipid molecules are required to form a complete annular shell around MscL. Assuming that all the lipid perturbation energy is concentrated in the annular shell of lipids around the protein, the perturbation energy per lipid molecule due to hydrophobic mismatch will be given by $\Delta G/29$. Equations 7 and 8 can be used to calculate lipid binding constants relative to that of the lipid giving optimal matching to the protein, as a function of the number of carbon atoms in the lipid fatty acyl chains. As shown in Figure 11, eq 8 predicts a much steeper dependence of the relative binding constant on chain length than observed experimentally. Similar results have been obtained with Ca^{2+}-ATPase and KcsA (*5*, *7*), both showing only a small dependence of the

binding constant on chain length. In contrast, the β-barrel protein OmpF shows a much steeper dependence of the binding constant on chain length, the variation in binding constant over the chain length range from C12 to C20 being close to that expected theoretically for a rigid protein (*17*). The observation that the rigid protein approach of Fattal and Ben-Shaul (*14*) works reasonably well for a β-barrel protein but not for the α-helical membrane proteins Ca^{2+}- ATPase, KcsA, and MscL suggests that α-helical membrane proteins should not be considered to be rigid in the sense of Fattal and Ben-Shaul (*14*). That is, whereas β-barrel proteins cannot distort to match the surrounding lipid bilayer, α-helical membrane proteins can. Distortion of α-helical membrane proteins to match the hydrophobic thickness of the surrounding lipid bilayer is consistent with the observation that the activities of many α-helical membrane proteins change with changing bilayer thickness (*6*−*12*).

The most likely distortion of an α-helical membrane protein to match the thickness of the surrounding lipid bilayer is a tilting of the transmembrane α-helices, although rotation of side chains for residues at the ends of the helices about the Cα−Cβ bonds linking the side chains to the polypeptide backbone could also contribute (*44*). Distortion of a membrane protein will be highly cooperative. The difference in lipid binding constants on changing the fatty acyl chain length from C16 to C24 is about 1.5 (Table 4), corresponding to a free energy difference of 1 kJ/mol of lipid, but ca. 29 kJ/mol of MscL, since MscL is surrounded by ca. 29 first-shell (annular) lipid molecules, sufficient to cause a significant change in conformation. Hydrophobic mismatch has, in fact, been shown to have a significant effect on the function of EcMscL, thin bilayers favoring channel opening and thick bilayers favoring a closed configuration (*45*). Studies of spin-labeled EcMscL are also consistent with changes in the conformation of EcMscL as a function of bilayer thickness although changes in channel structure between phospholipids with chain lengths of C18 and C14 are small (*45*, *46*).

Effects of the Phospholipid Headgroup. The binding constant for di(C18:1)PE relative to di(C18:1)PC for TbMscL is close to 1 (Table 5), showing no significant selectivity in binding. Phosphatidylcholine and phosphatidylethanolamine have also been shown to bind with equal affinity to the porin OmpF (*17*), whereas for KcsA and Ca^{2+}-ATPase the affinity for phosphatidylethanolamine is about half that for phosphatidylcholine (*7*, *31*). Binding constants for di(C18:1)PG and di(C18:1)PS to TbMscL are about double that for di(C18:1)PC in the presence of 100 mM KCl (Table 5). Similarly, the binding constant for tetra(C18:1)CL is about double that for di(C18:1)PC when the concentrations of phospholipid are expressed on a chain basis (Table 5). The relative binding constant for di(C18:1)PS decreases with increasing ionic strength, being close to 1 in 1 M KCl (Table 5), suggesting a large charge component in the anionic lipid−protein interaction. Results for phosphatidic acid are significantly different from those observed with the other anionic phospholipids (Table 5). The quenching profiles observed with phosphatidic acid (Figure 6) are consistent with two classes of binding sites on TbMscL for di(C18:1)PA, the affinity for di(C18:1)PA being about double that for di(C18:1)PC at one class of sites but 3.5-fold greater at the second class of sites (Table 5). The effects of ionic strength are much smaller on the binding of phosphatidic acid than on the binding of phosphatidylserine (Table 5), suggesting that interactions other than charge interactions are important in the binding of the small phosphatidic acid headgroup to TbMscL.

The major membrane lipids of the *Mycobacteria* are the anionic phospholipids cardiolipin and phosphatidylinositol-mannosides, with the zwitterionic phospholipid phosphatidylethanolamine making up about a third of the total phospholipid (*43*). Thus, given the slightly stronger binding of anionic than zwitterionic phospholipids to TbMscL (Table 5), the majority of the lipids surrounding TbMscL in the native membrane are likely to be anionic phospholipids. In contrast, the major phospholipid in the cytoplasmic membrane of *E. coli* is phosphatidylethanolamine, with 24 mol % phosphatidylglycerol and 4 mol % cardiolipin (*47*). Thus, if binding constants for anionic phospholipids for EcMscL are similar to those for TbMscL, then the lipid environment for EcMscL in the native membrane will be enriched in phosphatidylethanolamine compared to that for TbMscL.

ACKNOWLEDGMENT

We thank Professor Martinac and Professor Rees for the generous gifts of the MscL constructs and Professor Booth for the generous gift of MJF465.

REFERENCES

1. Jones, M. R., Fyfe, P. K., Roszak, A. W., Isaacs, N. W., and Cogdell, R. J. (2002) *Biochim. Biophys. Acta 1565*, 206−214.
2. Lange, C., Nett, J. H., Trumpower, B. L., and Hunte, C. (2001) *EMBO J. 20*, 6591−6600.
3. Valiyaveetil, F. I., Zhou, Y., and MacKinnon, R. (2002) *Biochemistry 41*, 10771−10777.
4. Tanford, C. (1980) *The Hydrophobic Effect: Formation of Micelles and Biological Membranes*, John Wiley, New York.
5. Williamson, I. M., Alvis, S. J., East, J. M., and Lee, A. G. (2002) *Biophys. J. 83*, 2026−2038.
6. Caffrey, M., and Feigenson, G. W. (1981) *Biochemistry 20*, 1949−1961.
7. East, J. M., and Lee, A. G. (1982) *Biochemistry 21*, 4144−4151.
8. Starling, A. P., East, J. M., and Lee, A. G. (1993) *Biochemistry 32*, 1593−1600.
9. Cornelius, F. (2001) *Biochemistry 40*, 8842−8851.
10. Pilot, J. D., East, J. M., and Lee, A. G. (2001) *Biochemistry 40*, 8188−8195.
11. Baldwin, P. A., and Hubbell, W. L. (1985) *Biochemistry 24*, 2633−2639.
12. Carruthers, A., and Melchior, D. L. (1984) *Biochemistry 23*, 6901−6911.
13. Mouritsen, O. G., and Bloom, M. (1984) *Biophys. J. 46*, 141−153.
14. Fattal, D. R., and Ben-Shaul, A. (1993) *Biophys. J. 65*, 1795−1809.
15. Nielsen, C., Goulian, M., and Andersen, O. S. (1998) *Biophys. J. 74*, 1966−1983.
16. London, E., and Feigenson, G. W. (1981) *Biochemistry 20*, 1939−1948.
17. O'Keeffe, A. H., East, J. M., and Lee, A. G. (2000) *Biophys. J. 79*, 2066−2074.
18. Webb, R. J., East, J. M., Sharma, R. P., and Lee, A. G. (1998) *Biochemistry 37*, 673−679.
19. East, J. M., Melville, D., and Lee, A. G. (1985) *Biochemistry 24*, 2615−2623.
20. Lee, A. G. (1977) *Biochim. Biophys. Acta 472*, 285−344.
21. Oakley, A. J., Martinac, B., and Wilce, M. C. J. (1999) *Protein Sci. 8*, 1915−1921.
22. Chang, G., Spencer, R. H., Lee, A. T., Barclay, M. T., and Rees, D. C. (1998) *Science 282*, 2220−2226.
23. Laemmli, U. K. (1970) *Nature 227*, 680−685.
24. Gutierrez-Merino, C., Munkonge, F., Mata, A. M., East, J. M., Levinson, B. L., Napier, R. M., and Lee, A. G. (1987) *Biochim. Biophys. Acta 897*, 207−216.

25. Bligh, E. G., and Dyer, W J. (1959) *Can. J. Biochem. Physiol. 37*, 911−915.
26. Bartlett, G. R. (1959) *J. Biol. Chem. 234*, 466−468.
27. Mall, S., Sharma, R. P., East, J. M., and Lee, A. G. (1998) *Faraday Discuss. 111*, 127−136.
28. Levina, N., Totemeyer, S., Stokes, N. R., Louis, P., Jones, M. A., and Booth, I. R. (1999) *EMBO J. 18*, 1730−1737.
29. Blount, P., Sukharev, S. I., Moe, P. C., Schroeder, M. J., Guy, H. R., and Kung, C. (1996) *EMBO J. 15*, 4798−4805.
30. Sukharev, S. I., Schroeder, M. J., and McCaslin, D. R. (1999) *J. Membr. Biol. 171*, 183−193.
31. Alvis, S. J., Williamson, I. M., East, J. M., and Lee, A. G. (2003) *Biophys. J.*, in press.
32. Warren, G. B., Toon, P. A., Birdsall, N. J. M., Lee, A. G., and Metcalfe, J. C. (1974) *Biochemistry 13*, 5501−5507.
33. Bolen, E. J., and Holloway, P. W. (1990) *Biochemistry 29*, 9638−9643.
34. Mall, S., Broadbridge, R., Sharma, R. P., East, J. M., and Lee, A. G. (2001) *Biochemistry 40*, 12379−12386.
35. Abrams, F. S., and London, E. (1992) *Biochemistry 31*, 5312−5322.
36. Lakowicz, J. R. (1999) *Principles of Fluorescence Spectroscopy*, Kluwer Academic/Plenum Press, New York.
37. Matko, J., Ohki, K., and Edidin, M. (1992) *Biochemistry 31*, 703−711.
38. Zelent, B., Kusba, J., Gryczynski, I., Johnson, M. L., and Lakowicz, J. R. (1996) *J. Phys. Chem. 100*, 18592−18602.
39. Lewis, B. A., and Engelman, D. M. (1983) *J. Mol. Biol. 166*, 211−217.
40. Sperotto, M. M., and Mouritsen, O. G. (1988) *Eur. Biophys. J. 16*, 1−10.
41. Landolt-Marticorena, C., Williams, K. A., Deber, C. M., and Reithmeier, R. A. F. (1993) *J. Mol. Biol. 229*, 602−608.
42. Ulmschneider, M. D., and Sansom, M. S. P. (2001) *Biochim. Biophys. Acta 1512*, 1−14.
43. Coren, M. B. (1984) in *The Mycobacteria* (Kubica, G. P., and Wayne, L. G., Eds.) pp 379−415, Marcel Dekker, New York.
44. Lee, A. G. (2003) *Biochim. Biophys. Acta 1612*, 1−40.
45. Perozo, E., Kloda, A., Cortes, D. M., and Martinac, B. (2002) *Nat. Struct. Biol. 9*, 696−703.
46. Perozo, E., Cortes, D. M., Sompornpisut, P., and Martinac, B. (2002) *Nature 418*, 942−948.
47. Harwood, J. L., and Russell, N. J. (1984) *Lipids in Plants and Microbes*, George Allen & Unwin, London.
48. Ladokhin, A. S. (1999) *Biophys. J. 76*, 946−955.
49. Esnouf, R. M. (1999) *Acta Crystallogr., Sect. D 55*, 938−940.

BI034995K